*International Journal Dental and Medical Sciences Research (IJDMSR)*
*ISSN: 2393-073X Volume 4, Issue 4 (April - 2020), PP 18-24*
***www.ijdmsr.com***

# Characterization of Non-Small Cell Lung Carcinoma Gross Target Volume with 18F-FDG PET scan using Texture Analysis

Sami Y. I. Awadain, Suhaib Alameen, Eman M. Algorashi,
Mohamed E. M. Gar-Elnabi
*College of Medical Radiologic Science, Sudan University of Science and Technology, Khartoum-Sudan*
**Corresponding author: Sami Y. I. Awadain*

**ABSTRACT:-** This study concern to characterize the lung area to cardiac, lung, tumor and submucosal using Gray Level Co-occurrence Matrix (GLCM) and extract classification features from PET/CT with fluorine-18 fluorodeoxyglucose images. Using the GLCM techniques to find the gray level variation in PET/CT images it complements the features extracted from PET/CT images with variation of gray level in pixels and estimate the distribution of the sub-patterns using Interactive Data Language IDL software. The results show's that the Gray Level Co-occurrence Matrix and features extracted give a classification accuracy of cardiac 91.6%, lung 100%, tumor 99.6%, while the sub-mucosal showed accuracy 91.2%. The overall classification accuracy of lung area 96.0%. These relationships are stored in a Texture Dictionary that can be later used to automatically annotate new PET/CT images with the appropriate lung area names.

**Keywords:-** Texture Analysis, Lung Carcinoma, PET scan, GLCM

## I. INTRODUCTION

18F-FDG PET/CT scan is a well-established hybrid-functional imaging technique for cancer evaluation in the clinical field.[18]F-FDG PET scan enables non-invasive tumor evaluation for grading, staging and measuring the response to treatment with only reflects the highest value of metabolic activity in a tumor, and volumetric parameters such as metabolic tumor volume only reflect overall tumor burden (1).

The conventional treatment strategy in advanced lung cancer was determined based on the simplified cancer type classification, namely, non-small cell lung carcinoma (NSCLC) and small cell carcinoma (SCLC), although NSCLC is a heterogeneous disease group including adenocarcinoma (ADC) and squamous cell carcinoma (SqCC). Recent advances in targeted anti-lung cancer agents emphasize certain sub-classifications of tumor type in NSCLC, especially in ADC (2). PET with $^{18}$F-FDG has been used in radiation treatment planning for non–small cell lung cancer (NSCLC). Thresholds of 15%–50% the maximum standardized uptake value ($SUV_{max}$) have been used for gross tumor volume (GTV) delineation by PET ($PET_{GTV}$), with 40% being the most commonly used value (3).

Noninvasive metabolic imaging of tumors may have complementary roles to histopathologic evaluation although the human eye is a good tool for discriminating the texture characteristics of a lesion, it has disadvantages, including being hard to achieve objectification. In addition, the visual system is able to recognize limited patterns of the texture. So the texture analysis based on a mathematical approach is a promising tool for recognizing hidden patterns of lesion for classification(2).

Histopathological characteristics of tumor may compose the gross texture of the tumor not only on the tissue, but also on the images. Previous researches have investigated the potential of texture analysis in anatomical imaging such as US, CT and MRI, and presented the data supporting the hypothesis that texture features on images can discriminate the tissue types.(4)

Texture analysis on $^{18}$F-fluorodeoxyglucose positron emission tomography ($^{18}$F-FDG PET) scan is a relatively new imaging analysis tool to evaluate metabolic heterogeneity. We analyzed the difference in textural characteristics between non-small cell lung carcinoma (NSCLC) subtypes, namely adenocarcinoma (ADC) and squamous cell carcinoma (SqCC) (2). The digital PET image is composed of voxels and each one has a value in the gray-level intensity of the volume element in space(5).

The gray-level intensity is a representative value of glucose metabolism within the 18F-FDG PET image, so gross texture of a lesion within the image may represent its histopathologic characteristics. Texture analysis is a mathematical pattern analysis technique and it quantifies the interrelationships of the pixels or voxels via complex and variable mathematical methods (6)

Prior studies have shown the relationship between SUVmax of 18F-fluorodeoxyglucose positron emission tomography (18F-FDG PET) scan and histopathologic diagnosis (7).

## II. SECOND-ORDER STATISTICAL TEXTURE ANALYSIS

The human visual system cannot discriminate between texture pairs with matching second order statistics (8). The first machine-vision framework for calculating second-order or pixel co-occurrence texture information was developed for analyzing aerial photography images (9).

In this technique pixel co-occurrence matrices, which are commonly referred to as grey-tone spatial dependence matrices (GTSDM), are computed. The entries in a GTSDM are the probability of finding a pixel with grey-level i at a distance d and angle α from a pixel with a grey-level j. This may be written more formally as P (i, j: d,α). An essential component of this framework is that each pixel has eight nearest-neighbors connected to it, except at the periphery. As a result four GTSDMs are required to describe the texture content in the horizontal ($H_P = 0^0$), vertical ($P_V=90^0$) right- ($P_{RD}=45^0$) and left diagonal ($P_{LD}= 135^0$) directions. This is illustrated in Figure. 1.

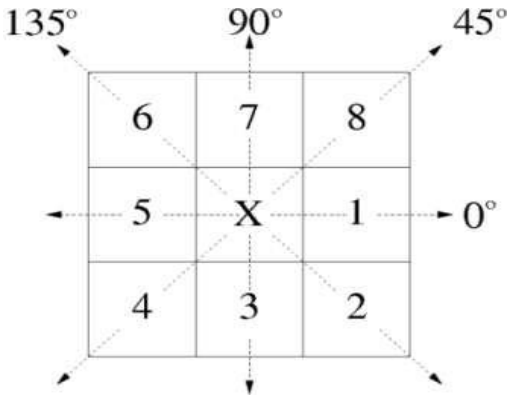


**Fig. 1. Eight nearest-neighbor pixels used in the GTSDM framework to describe pixel connectivity. Cells 1 and 5 show the horizontal ($H_P$), 4 and 8 the right-diagonal ($P_{RD}$), 3 and 7 the vertical ($P_V$) and 2 and 6 the left-diagonal ($P_{LD}$) nearest-neighbors (9).**

An example of the calculation of a horizontal co-occurrence matrix (**$H_P$**) on a 4x4 image containing four unique grey-levels is shown in Fig. 2. A complete representation of image texture is contained in the co-occurrence matrices calculated in the four directions. Extracting information from these matrices using textural features, which are sensitive to specific elements of texture, provides unique information on the structure of the texture being investigated. Haralick et al., proposed a set of 14 local features specifically designed for this purpose (9).

In practice the information provided by certain features may be highly correlated or of limited practical use. A feature selection strategy is therefore useful with this approach to take account of redundant, or irrelevant, information. It is also interesting to note that prior to any processing the GTSDMs, which are symmetric, can provide some useful information on the characteristics of the image being studied. For example, the co-occurrence matrix entries for a coarse texture will be heavily focused along the diagonals relative to the distance d between the pixels studied.

| | | | |
|---|---|---|---|
| 0 | 2 | 2 | 2 |
| 0 | 3 | 2 | 2 |
| 1 | 2 | 2 | 2 |
| 3 | 0 | 3 | 0 |

$(P_H)$

| Grey-Level | 0° | 0 | 1 | 2 | 3 |
|---|---|---|---|---|---|
| | 0 | 0 | 0 | 1 | 4 |
| | 1 | 0 | 0 | 1 | 0 |
| | 2 | 1 | 1 | 10 | 1 |
| | 3 | 4 | 0 | 1 | 0 |

**Fig. 2. Simple example demonstrating the formation of a co-occurrence matrix from an image. Left, 4x4 image with four unique grey-levels. Right, the resulting horizontal co-occurrence matrix ($P_H$).**

## III. METHODOLOGY:

**PET/CT System Description:** The Discovery™ PET/CT consist of a fully integrated 3D Positron Emission Tomography and multi-slice Computed Tomography scanner with all available CT diagnostic applications, except gantry tilt. Due to the overall length of the PET/CT, the patient table sits on a special base that drives the table between the PET and CT portions of the gantry. The PET/CT table is rated for a patient

weight of 227 Kg (500 pounds) and the cradle travels up to 1700mm on standard systems, or up 2 meters on systems with the 2m scan range option.

**Procedures:**

PET/CT study for 156 patients were examined in Kuwait Cancer Control Center by 18F-FDG Whole-Body PET/CT. were the patients received an intravenous injection of 4.4 mCi of 18F-FDG. After an initial uptake phase of an approximately 65 minutes, a CT-Scan without oral contrast without IV contrast, without breath holding at low mA level was acquired for attenuation correction and localization purposes only. Arms were held up. Subsequently PET images from the vertex to mid-thigh were obtained. CT, PET and fused images were reconstructed in trans-axial, coronal and sagittal projections and interpreted from a workstation. Patient's plasma glucose is 5.2 mmol/l.

## IV. RESULTS AND DISCUSSION:

The features extracted from PET/CT images using Second order statistic and All these features were calculated for all images and then the data were ready for discrimination which was performed using step-wise technique in order to select the most significant feature that can be used to classify the lung cells from PET/CT images and the results show that:

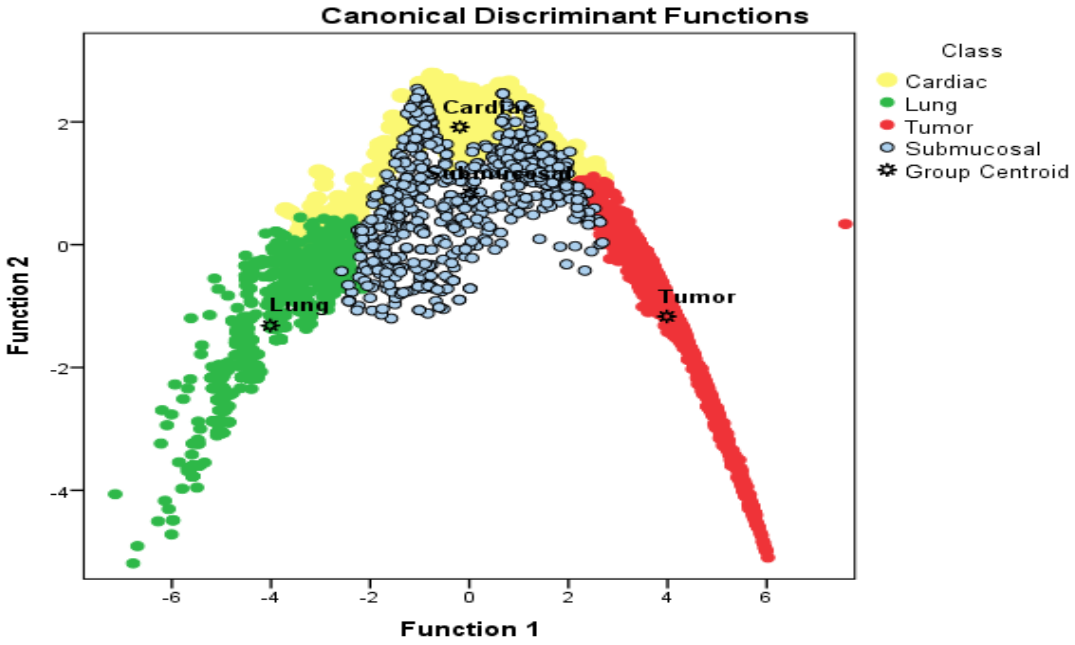


**Fig .3 Scatter plot generated using discriminate analysis function for four classes represents: Cardiac, lung, tumor, submucosal**

The classification showed that the lung cells were classified well from the rest of the tissues although it has characteristics mostly similar to surrounding tissue.

**Table 1: Showed the classification accuracy of the lung cells using linear discriminant analysis:**

| Classes | | Predicted Group Membership | | | | Total |
|---|---|---|---|---|---|---|
| % | Original groups | Cardiac | Lung | Tumor | Submucosal | |
| | Cardiac | 91.6 | 7.4 | 0.1 | 0.9 | 100.0 |
| | Lung | 0.0 | 100.0 | 0.0 | 0.0 | 100.0 |
| | Tumor | 0.1 | .0 | 99.6 | 0.4 | 100.0 |
| | Submucosal | 4.8 | 3.7 | 0.3 | 91.2 | 100.0 |

**96.0% of original grouped cases correctly classified**

Table (1) show classification score matrix generated by linear discriminate analysis and the overall classification accuracy of lung cells 96.0%, were the classification accuracy of cardiac 91.6%, lung accuracy 100%, the tumor 99.6%, While the submucosal showed a classification accuracy of 91.2%.

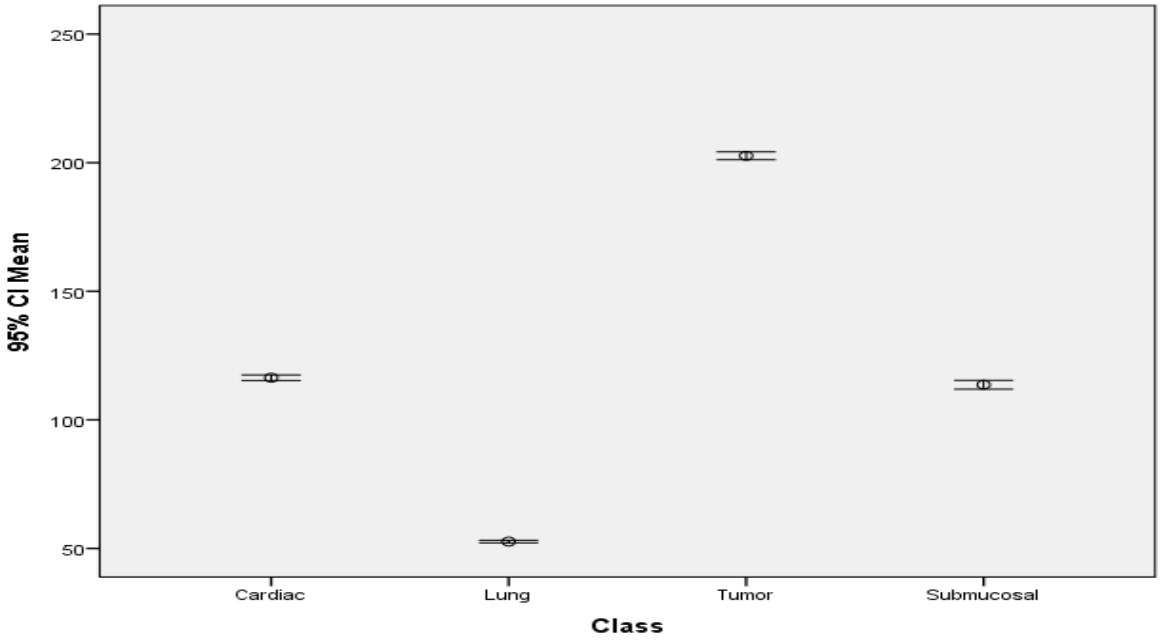


**Fig 4. Show error bar plot for the CI mean textural features that selected by the linear stepwise discriminate function to discriminates between all features. From the discriminate power point of view in respect to the applied features the mean can differentiate between all the classes successfully.**

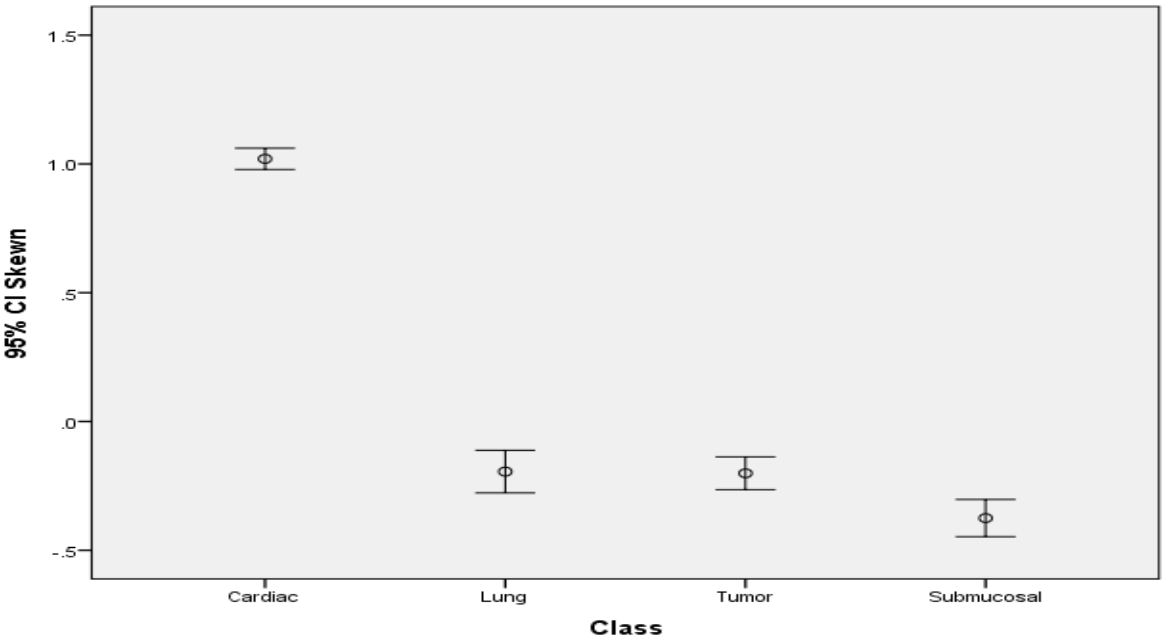


**Fig 5. Show error bar plot for the CI skewness textural features that selected by the linear stepwise discriminate function to discriminates between all features. From the discriminate power point of view in respect to the applied features the skewness can differentiate between all the classes successfully.**

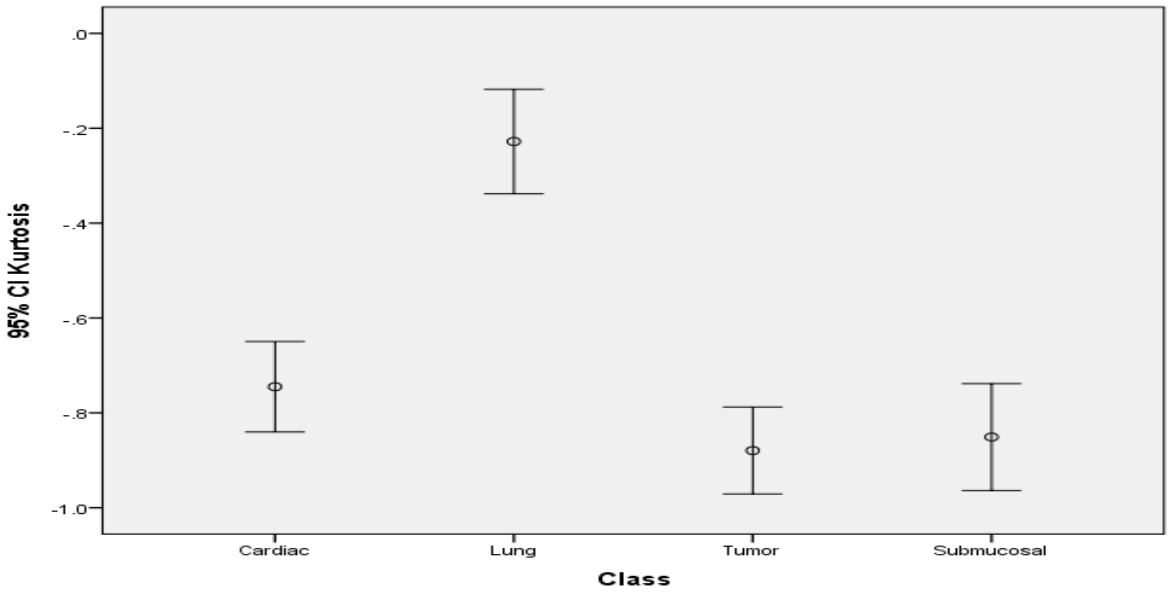


**Fig 6. show error bar plot for the CI kurtosis textural features that selected by the linear stepwise discriminate function as a discriminate feature where it discriminate between all features.**

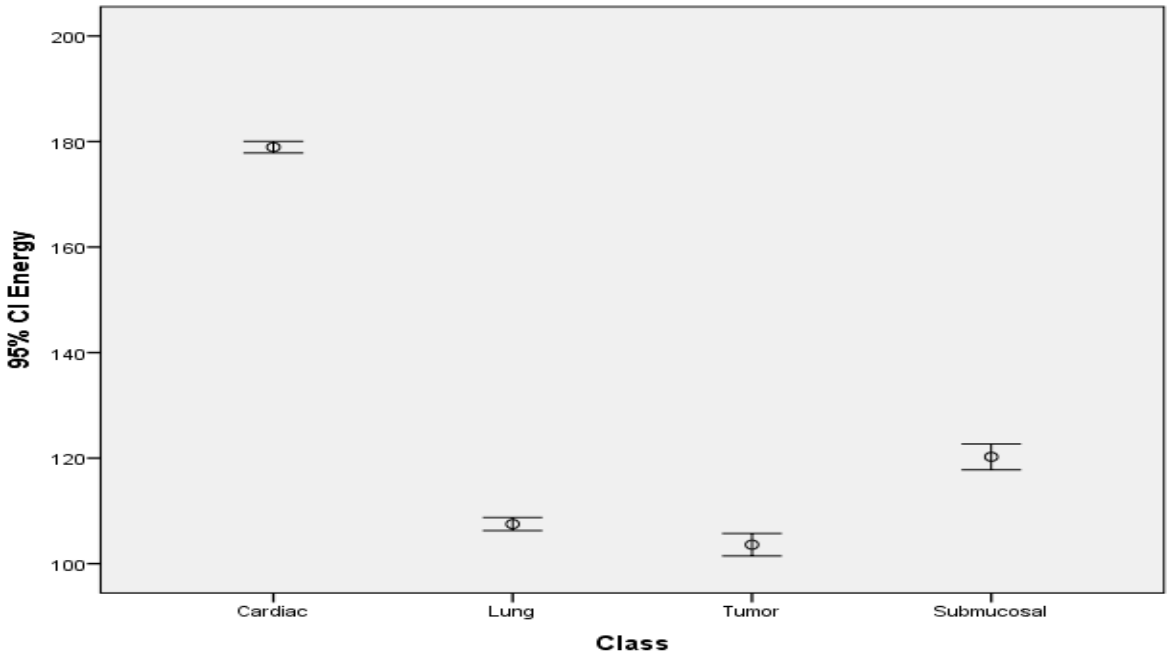


**Fig 7. Show error bar plot for the CI energy textural features that selected by the linear stepwise discriminate function where it discriminate between all features.**

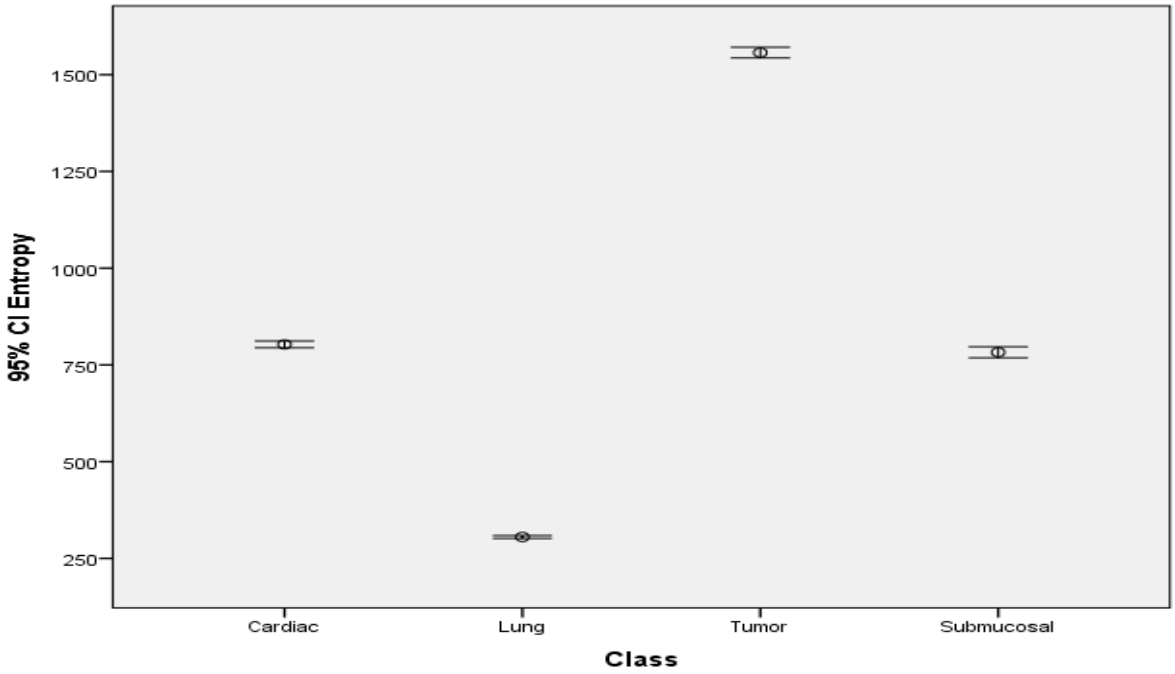


**Fig 8. show error bar plot for the CI entropy textural features that selected by the linear stepwise discriminate function as a discriminate feature between all features.**

From the discriminate power point of view in respect to the applied features the entropy can differentiate between all the classes successfully. comparable with previous study in texture analysis; Suhaib Alameen et al 2017 [10], Characterization of Hepatocellular Carcinoma in CT Images using Gray Level Run Length Matrix Several texture features are introduced from (GLRLM) and the classification accuracy of hepatocellular carcinoma 98.8%, liver accuracy 85.2 %, While the spine and ribs showed a classification accuracy of 75.3 % respectively. Total classification accuracy 85.4%

Einas M. Ahmed 2017 [11] discussed the assessment of Quality Control Uniformity & linearity of SPECT Gamma Camera using Image Processing, and the result showed that the resolution for minimum object used 4mm was 70% and increased with object size increased to reach 100% resolution for an object size of 10 mm i.e. 100% resolution corresponds to the coordinate of the MTF at 10% and frequency of 0.05cycle /mm. Inconclusion the developed algorithm can be used objectively and improved as required without looking for expertise from other country, as well it can be made to check the acceptance of the device performance regardless the built-in programs.

Texture analysis depending on the relative attenuation coefficient of tissues and can used to avoid invasive technique if the base line for individual tissues being determined and algorithmic aided computer have been applied.

## V. CONCLUSION:

The classification processes of non-small cell lung carcinoma gross target volume with fluorine-18 fluorodeoxyglucose in KCCC were defining the lung area to cardiac, lung, tumor and submucosal and carried out using Interactive Data Language (IDL) program as platform for the generated codes. The result of the classification showed that the lung tissues were classified well from the rest of the tissues although it has characteristics mostly similar to surrounding tissue.

Several texture features are introduced from Gray Level Co-occurrence Matrix (GLCM) and the classification score matrix generated by linear discriminate analysis and the overall classification accuracy of image regions 96%, and the classification accuracy of cardiac 91.6%, lung 100%, tumor 99.6%, while the submucosal showed accuracy 91.2%.

Using Linear discrimination analysis generated a classification function which can be used to classify other image into the mention classes as using the following multi regression equation;

Cardiac = (Mean * 11.905) +(Skewness * -3.887) + (Energy *-0.004) + (Entropy * 1.363) - 145.247
Lung = (Mean * 9.401) +( Skewness * -4.229) + (Energy *-0.034) + (Entropy * 1.344) -81.525
Tumor = (Mean * 11.964) +( Skewness * -3.968) + (Energy *-0.104) + (Entropy * 1.344) - 162.757
Sub-mucosal = (Mean * 12.565) + ( Skewness * -5.213) + (Energy *-0.079) + (Entropy * 1.441) - 147.494

**REFRENCES:**


[1]. Ha S, Choi H, Cheon GJ, Kang KW, Chung J-K, Kim EE, et al. Autoclustering of non-small cell lung carcinoma subtypes on 18 F-FDG PET using texture analysis: a preliminary result. Nuclear medicine and molecular imaging. 2014;48(4):278-86.

[2]. Jung K-W, Park S, Kong H-J, Won Y-J, Lee JY, Seo HG, et al. Cancer statistics in Korea: incidence, mortality, survival, and prevalence in 2009. Cancer research and treatment: official journal of Korean Cancer Association. 2012;44(1):11.

[3]. Biehl KJ, Kong F-M, Dehdashti F, Jin J-Y, Mutic S, El Naqa I, et al. 18f-fdg pet definition of gross tumor volume for radiotherapy of non–small cell lung cancer: Is a single standardized uptake value threshold approach appropriate? Journal of Nuclear Medicine. 2006;47(11):1808-12.

[4]. Ba-Ssalamah A, Muin D, Schernthaner R, Kulinna-Cosentini C, Bastati N, Stift J, et al. Texture-based classification of different gastric tumors at contrast-enhanced CT. European journal of radiology. 2013;82(10):e537-e43.

[5]. Castellano G, Bonilha L, Li L, Cendes F. Texture analysis of medical images. Clinical radiology. 2004;59(12):1061-9.

[6]. Rahim MK, Kim SE, So H, Kim HJ, Cheon GJ, Lee ES, et al. Recent trends in PET image interpretations using volumetric and texture-based quantification methods in nuclear oncology. Nuclear medicine and molecular imaging. 2014;48(1):1-15.

[7]. Han B, Lin S, Yu L-j, Wang R-z, Wang Y-y. Correlation of 18F-FDG PET activity with expressions of survivin, Ki67, and CD34 in non-small-cell lung cancer. Nuclear medicine communications. 2009;30(11):831-7.

[8]. Julesz, B. (1975). Experiments in the visual perception of texture. Scientific American, Vol. 232, pp 34-43.

[9]. Haralick, R.M.; Shanmugam K. & Dinstein, I . Texture features for image classification. I EEE Transactions on Pattern Analysis and Machine Intelligence, Vol. SMC-3, No. 6, Nov 1973, 610-621

[10]. Suhaib Alameen, Mohamed E. M. Gar-Elnabi, Wadah Ali, Characterization of Hepatocellular Carcinoma in CT Images using Gray Level Run Length Matrix, International Journal of Computer Application, Volume 7– No.2, March - April 2017 – PP 21-29

[11]. Einas M. Ahmed, Suhaib Alameen, YousraKhairi, Mohamed E. M. Gar-Elnabi, Assessment of Spatial Resolution on SPECT using Image Processing, IOSR Journal of Applied Physics, Volume 9, Issue 3 Ver. II 2017, PP 52-56


***Corresponding author: Sami Y. I. Awadain***
***College of Medical Radiologic Science, Sudan University of Science and Technology, Khartoum-Sudan***